

ELECTRONIC SUPPORTING INFORMATION

Light-activated gating and permselectivity in interfacial architectures combining “caged” polymer brushes and mesoporous thin films

Annette Brunsen, Jiayi Cui, Marcelo Ceolín, Aránzazu del Campo, Galo J.A.A. Soler-Illia and Omar Azzaroni

Synthesis of mesoporous amino-silica thin films.

Propylamino-functionalized mesoporous thin films were synthesized via co-condensation of the oxide precursor tetraethoxysilane (TEOS, Merck) and the amine precursor 3-aminopropyltriethoxysilane (APTES, Fluka 98%) in the presence of the template (F127 block copolymer, Aldrich, $M_w \sim 13600$).¹ The precursor solution was prepared using 0.8 TEOS:0.2 APTES:0.005 F127:24 EtOH:5.2 H₂O:0.28 HCl. This solution was used to produce films by dip-coating on glass and ITO substrates under 40-50% relative humidity conditions at 25 °C (1-2 mm s⁻¹ withdrawing speed). The organic template was removed by extraction in 0.01 mol dm⁻³ HCl in absolute ethanol (Merck) for 3 days under stirring.

Synthesis of 2-[(4,5-dimethoxy-2-nitrobenzoyl)aminoethyl methacrylate (NVOCAMA) monomer.

To a solution of 2-isocyanatoethyl methacrylate (6.2 g, 40 mmol) and 4,5-dimethoxy-2-nitrobenzyl alcohol (8.52 g, 40 mmol) in 150 ml dry THF, 0.40 mL of dibutyltin dilaureate (DBTL) was added and the mixture was allowed to react at room temperature for 3 h. The solvent was removed under reduced pressure, and the residue was purified by column chromatography on silica gel (dichloromethane/ethyl acetate (10/1, v/v) as eluent) at first and resultant raw product were further purified by recrystallization in ethanol and then in toluene. 11.8 g of product was obtained as yellow solid (yield 80%). ¹H NMR (250 MHz, CDCl₃, δ): 1.92 (s, 3H, CH₃), 3.49-3.56 (q, 2H, NHCH₂), 3.94 (s, 3H, OCH₃), 3.95 (s, 3H, OCH₃), 4.22-4.26 (t, 2H, OCH₂), 5.21 (s, 1H, NH), 5.49 (s, 2H, OCH₂), 5.57-5.59 (m, 1H, C=CH₂), 6.09(s, 1H, C=CH₂), 6.98 (s, 1H, Ar H), 7.68 (s, 1H, Ar H). ¹³C NMR (62.5 MHz, CDCl₃, δ): 18.29, 40.43, 56.41 (2C, OCH₃), 63.62, 63.71; 126.16, 135.90 (2C, CH₂=C); 108.17, 110.33, 127.89, 139.89, 148.16, 153.49 (6C, Ar), 155.87, 167.32 (2C, C=O). EIMS *m/z*: 367.4 [M⁺ - H].

Preparation of initiator-modified mesoporous films for ATRP.

Amino-silica mesoporous films were immersed into a solution of 37 μL of 2-bromisobutylryl bromide (BIB) and 41 μL of Et₃N in 4 mL of dried CH₂Cl₂ under N₂ for 30 min. After washing with dry CH₂Cl₂ and ethanol, the substrates were used for polymerization immediately.

Surface-initiated atom transfer radical polymerization (SI-ATRP) of PNOCAMA brushes from initiator-modified mesoporous silica films.

PNOCAMA (1.0 g, 2.5 mmol), CuBr (5.1 mg, 0.036 mmol), and CuBr₂ (0.8 mg, 0.0036 mmol) were added into 4 mL DMSO at 90 °C and degassed by passing a continuous stream of dry nitrogen through the solution while stirring for 15 min. PMDETA (22 μL, 0.1 mmol) was then added and the solution was degassed for a further 15 min. Initiator-coated substrates were sealed in reaction vessels, degassed, and left at 90 °C under nitrogen. The polymerization solution was then injected into vessel so that substrates were completely covered by the solution. After 3 hours of polymerization samples were removed, washed with CH₂Cl₂ and ethanol, and dried under a stream of nitrogen. The substrates were stored in the dark until use.

Light exposure of the PNOCAMA brush-modified mesoporous silica films.

Irradiation experiments were carried out using monochromatic light with a PolychromeV system (TILL Photonics GmbH, Grafelfing, Germany) at 365 nm (4.7 μW cm⁻²). After irradiation, substrates were washed with CH₂Cl₂ and rinsed with Milli-Q water

Environmental ellipsometric porosimetry.

Pore-ellipsometry studies were performed using a Sopra GES 5 spectroscopic ellipsometer with environmental control. This experimental setup allows for variable-angle broadband spectroscopic ellipsometry covering a spectral range from 210 nm to 900 nm. Film thickness and refractive index values were obtained from the ellipsometric parameters ψ and Δ under nitrogen flux containing variable water vapor quantities; P/P_{sat} was varied from 0 to 1 (P_{sat} being the saturation water vapor at 298 K). Film pore volume and pore size distribution at each P/P_{sat} were obtained by modeling the refractive index obtained according to a three-medium Bruggeman effective medium approximation (BEMA); pore size distributions were obtained from the analysis of the refractive index variation, using the WinElli 2 software (SOPRA, Inc.). In agreement with XRR data (Fig. 2c), pore ellipsometry also reveals that modification of mesoporous films with PNOCAMA brushes does not alter significantly the pore size of the films, *i.e.*: polymerization did not occur within the pore environment. As expected, this observation is also consistent with ellipsometric results from “uncaged” PAMA-modified mesoporous films (Fig. S1).

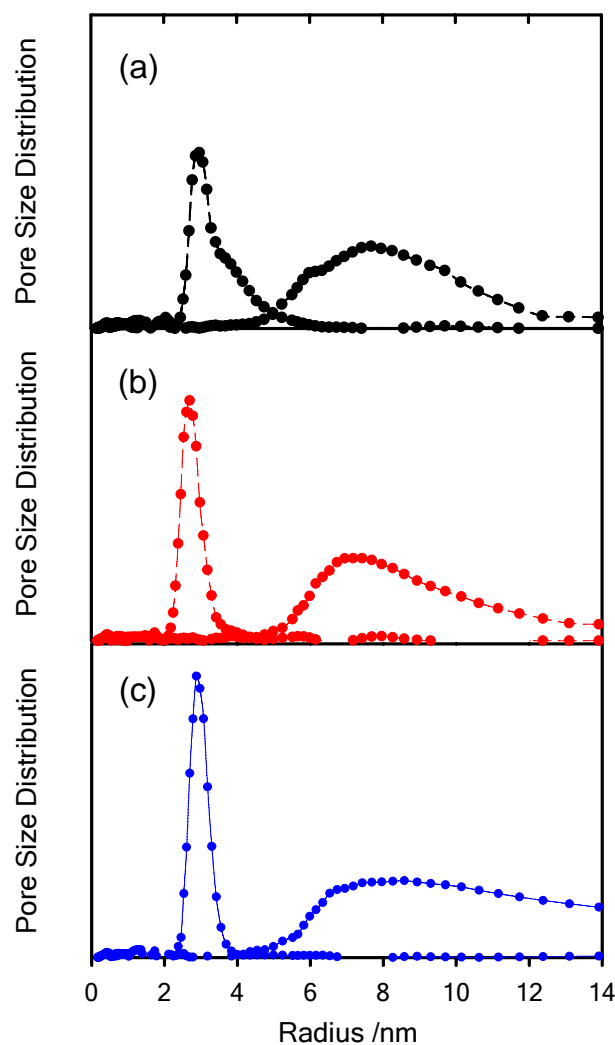


Figure S1. Pore size distribution of (a) amino-silica mesoporous film, (b) “caged” PNVOCAMA-modified mesoporous silica film and (c) “uncaged” PAMA-modified mesoporous silica film.

X-ray reflectivity (XRR) and grazing-incidence small-angle X-ray scattering (GISAXS) measurements.

XRR and GISAXS measurements were performed at the D10A-XRD2 beamline of Laboratório Nacional de Luz Síncrotron (Campinas, Brazil). The working wavelength was 0.16124 nm. In order to obtain accurate density values, measurements were performed under low-humidity conditions (under a stream of dry nitrogen). This is a relevant experimental aspect, as the condensation of atmospheric moisture within the pores could lead to a severe underestimation of the film mesoporosity. XRR measurements of amino-silica, PNVOCAMA-modified (“caged”) and PAMA-modified (“uncaged”) silica films evidenced no significant changes in the critical angle (Fig. 2c). This experimental evidence would suggest that polymerization did not take place within the mesopores. However, a detailed analysis of the corresponding Kiessig fringes, revealed the presence of an overlayer of 6 nm and 4 nm

in the case of PNVOCAAMA-modified and PAMA-modified mesoporous films, respectively. To this end, the reflectivity curves were analyzed by Fourier inversion of the data following the procedure described by Gibaud² and Goorsky.³ By performing a Fourier inversion of the reflected intensity divided by the Fresnel reflectivity, one can access to the autocorrelation function of the derivative of the electron density (or Patterson function). Fourier transforms of X-ray reflectivity scans from multi-layer structures provide useful layer thickness information. This approach has proved to be very effective at extracting layer thickness information from multi-layer structures that produce complicated specular x-ray reflectivity scans.⁴ The Fourier transform produces a series of sharp peaks that originate from different layer thicknesses. The peaks represent the combination of different layer thicknesses and the thickness of each layer can be determined from the computed Fourier transform.⁵

On the other hand, GISAXS characterization also confirmed that the photodeprotection process did not promote changes in the mesostructure of the hybrid film upon irradiation with UV light (Fig. S2).

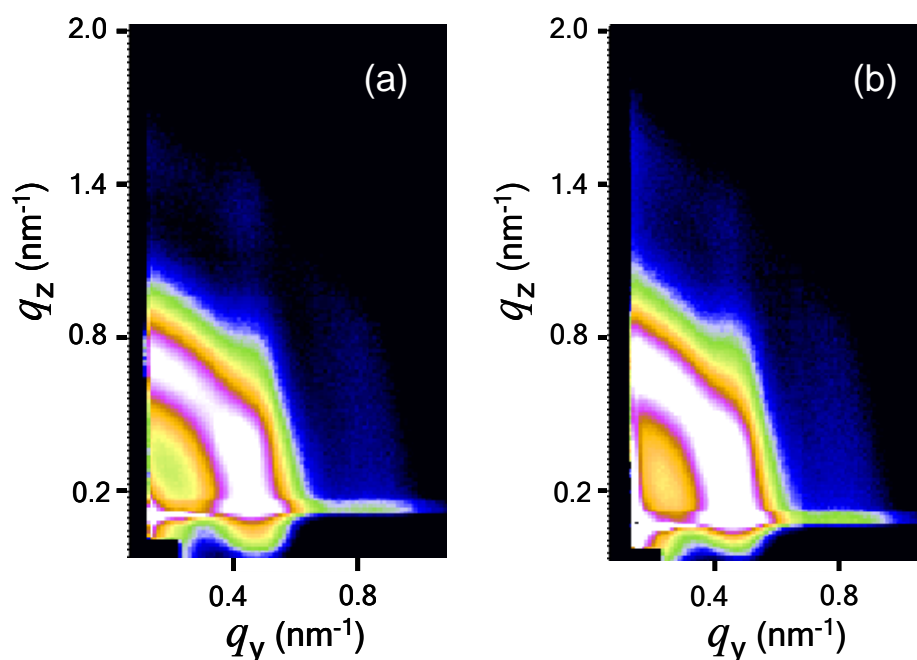


Figure S2. GISAXS patterns corresponding to a PNVOCAAMA-modified mesoporous film prior to (a) and after (b) irradiation.

Electrochemical probing of mass transport through the hybrid mesoporous film.

Cyclic voltammetry (CV) was used to analyze the change in the transport properties of electrochemical probes, anionic $\text{Fe}(\text{CN})_6^{3-}$ and cationic $\text{Ru}(\text{NH}_3)_6^{3+}$, prior to and after the “uncaging” process. As recently demonstrated by Walcarius and co-workers,⁶ changes in the voltammetric response of mesoporous electrodes reflect the changes in probe concentration or diffusion in response external

stimuli or the architecture of the pores. To this end, mesoporous films modified with caged polymer brushes were prepared on bare ITO electrodes (Fig. S3).

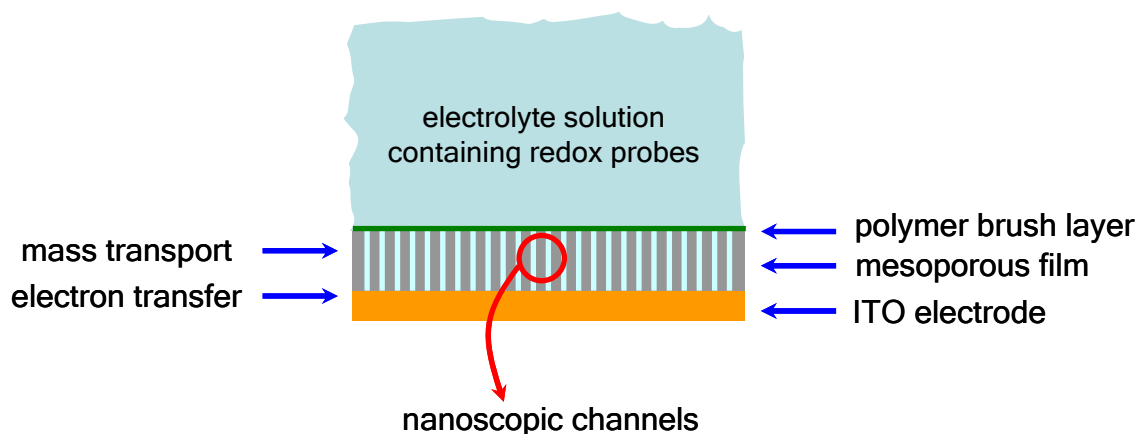


Figure S3. Simplified scheme of the hybrid mesostructured electrode used to monitor the mass transport of redox probes through the mesoporous film.

REFERENCES

- ¹ A. Calvo, P. C. Angelomé, V. M. Sánchez, D. A. Scherlis, F. J. Williams and G. J. A. A. Soler-Illia, Mesoporous Aminopropyl-Functionalized Hybrid Thin Films with Modulable Surface and Environment-Responsive Behavior, *Chem. Mater.*, 2008, **20**, 4661–4668.
- ² A. Gibaud and S. Hazra, X-ray reflectivity and diffuse scattering, *Curr. Sci.* 2000, **78**, 1467-1477.
- ³ B Poust and M. Goorsky, Enhanced Fourier Transforms for X-Ray Scattering Applications in “*Fourier Transforms – Approach to Scientific Principles*” edited by G. Nikolic (InTech, Vienna, 2011), Ch 17, pp. 321-340.
- ⁴ F. Bridou and B. Pardo, Grazing X-Ray Reflectometry Data Processing by Fourier Transform, *J. X-Ray Sci. Technol.* 1994, **4**, 200-216.
- ⁵ A. Gibaud, and G. Vignaud, Specular Reflectivity from Smooth and Rough Surfaces. *Lect. Notes Phys.* 2009, **770**, 85–131.
- ⁶ A. Walcarius and A. Kuhn, A. Ordered porous thin films in electrochemical analysis, *Trends Anal. Chem.* 2008, **27**, 593-603.